RSC Advances

ROYAL SOCIETY OF CHEMISTRY

www.rsc.org/advances

Cite this: DOI: 10.1039/c0xx00000x

www.rsc.org/xxxxxx

ARTICLE TYPE

Synergy Effect of C, Ag-Codoped TiO_2 Photocatalyst Within the GGA+U Framework

Meili Guo[a,*]

The electronic states and optical properties of the C, Ag-codoped TiO_2 were investigated within the GGA+U framework. Different doping concentration and different dopants distance (C_sAg_s (near and far), $C_{2s}Ag_s$ (near and far), and $C_{3s}Ag_s$ (near and far)) models were constructed. According to the formation energy results of these codoping systems, it was found that the low concentration codoping was more stable than the high concentration codoping. Therefore, we chose the C_sAg_s (near and far) codoped TiO_2 to calculate the further electronic structures and optical properties. It was found that the near distance codoping could narrow gap up to 2.81 eV, and the far distance codoping decreased the band gap up to 2.66 eV. Meanwhile, it was found that the far distance codoping preferred to form more localized states near the top of valance band, while the near distance codoping could induce more significant hybrid states during the gap. Optical properties showed that the C and Ag codoping could induce synergy effect compared with the single C and single Ag doping. After codoping, the visible absorption was stronger both for the near and far distance codoping than that of the single doping, moreover, the far distance codoping configuration could induce both of more significant band edge shift and stronger visible optical absorption than that of the near distance codoping configuration.

* E-mail: meiliguo314@163.com

Cite this: DOI: 10.1039/c0xx00000x

www.rsc.org/xxxxxx

ARTICLE TYPE

Introduction

TiO_2 is a highly efficient photocatalytic material for energy and environmental applications due to its strong oxidizing power, high chemical inertness, low cost, and long-term stability.[1-3] Unfortunately, the band gap of TiO_2 is large (3.2 eV for anatase and 3.0 eV for rutile structure), and only absorb very little visible light, which prevents its wide application in visible region.[4] To utilize the solar light, it is necessary to enhance the visible optical absorption of TiO_2.

The band gap narrowing and introducing gap states are two effective routes to improve visible optical absorption of TiO_2. Nonmetal doping can create the electronic states near the valence band or behave as a part of valance band, and thus can narrow the band gap of TiO_2.[5-8] For example, N doping is an effective route to create the N 2*p* electronic states near the top of valence band, and lots of experiments also confirmed the enhancement of visible light response of N-doped TiO_2.[9-15] In addition, C-doped TiO_2 has showed the 0.12-0.3 eV 2*p* electronic states near the top of valence band, and X-ray photoelectron spectroscopy showed an increased electron density of states above the valence band of TiO_2.[16-18] As a contrast, metal doping prefers to produce the electronic states in the band gap, and thus induce the visible optical absorption centre.[19-21] It has also been shown that metal-doped TiO_2 can perform the visible photocatalytic properties.[22-23]

Due to the individual benefit of metal and nonmetal doping, it has been proposed that metal and nonmetal codoping can combine the two benefits and thus can induce some interesting results.[24] It was reported that codoping could improve the photoactivity of TiO_2 by gap states and band gap narrowing.[24-29] For example, Gai et al calculated the band structure and electronic stated density of metal and nonmetal codoped TiO_2 in detail, and they predicted C, Mo-codoped TiO_2 could be conceived as a visible photocatalysts.[28] Band edges of TiO_2 could be modified by passivated C, Mo codopants to shift the valence band edge up significantly, while leaving the conduction band edge almost unchanged, thus satisfying the stringent requirements. Subsequently, the experiment confirmed that C, Mo codoping could enhance photocatalytic activity of TiO_2.[30] In another independent work, Zhu et al reported that noncompensated n-p codoping presented effectively narrow the band gap, and N, Cr codoping could be a good candidate for enhancing visible photoactivity of TiO_2.[31-32]

In addition, atom configuration can play a very important role in codoping system. For codoping system, the far distance configuration for doping atoms can avoid the formation of hybrid electronic states,[33] and will be benefit to band gap engineering. However, sometimes, some hybrid electronic states caused by the near distance doping could form some special structures which could induce some unexpected optical phenomenon and thus improved the visible photoactivity.[34] For example, the N, B-codoped system, the electronic states at the top of valence band and in the band gap will be significant different for different doping distance.[35-36] Besides, it was reported that the distance of doping atoms in carbon nanotubes had a significant effect on electronic structure.[37] Thus, we conceived that different doping configuration will have a significant influence on electronic structure and optical properties of codoped TiO_2, which can provide some information for develop visible phtocatalytic and water splitting materials. In this work, in order to guarantee the reliability of the results, we constructed models with different doping concentration and different dopants distance (C_sAg_s (near and far), $C_{2s}Ag_s$ (near and far), and $C_{3s}Ag_s$ (near and far)), however, the formation energy results indicated the configuration with high codoping concentration was unstable. Therefore, we presented the electronic structures and optical properties of C, Ag-codoped anatase TiO_2 with the low doping concentration (C_sAg_s (near and far)). Meanwhile, the GGA+U method was employed to correct the band gap.

Computational Methods

All the calculations were based on the density functional theory (DFT), within the plane-wave-pseudo-potential approach, together with the Perdew-Burke-Ernzerhof (PBE) exchange correlation functional.[38-39] The interaction between valence electrons and the ionic core was described by ultrasoft pseudopotential, which was used with $2s^22p^4$, $3d^24s^2$, $2s^22p^2$ and $4d^{10}5s^1$ as the valence electrons configuration for the O, Ti, C, and Ag atoms, respectively. We chose the energy cutoff to be 340 eV for the pure and C, Ag-codoped TiO_2 systems. The Brillouin-zone sampling mesh parameters for the k-point set were 1×2×2.[40]

Firstly, geometry optimization was performed by GGA method, because the geometry parameters calculated by the GGA method are closer to the experiments than the GGA+U method.[41] In this way, atomic positions and lattice parameters were optimized. The equilibrium lattice constants and fractional atomic coordinates are deduced from the total-energy minimization by using the BFGS geometry optimization method. Relaxation of the lattice parameters and atomic positions is carried out under the constraint of the unit-cell space group symmetry. Energy–volume relations are obtained by varying unit-cell volume and the fitted results are obtained using the Murnaghan equation of state:

$$E_{tol} = \frac{B_0 V}{B_0'}\left[\left(\frac{V_0}{V}\right)^{B_0'}\left(\frac{1}{B_0'-1}\right)+1\right]+E_0$$

From the fitted results, the estimate of the static bulk modulus B_0 at zero pressure, and the first-order pressure derivative of the bulk modulus B_0' are obtained. In the optimization process, the energy change, maximum force, maximum stress and maximum

displacement tolerances are set as 2×10^{-5} eV/atom, 0.05 eV/Å, 0.1 GPa and 0.002 Å, respectively.

And then, the electronic structure and optical properties of C, Ag-codoped TiO_2 were performed using GGA+U method.[42] The GGA+U approach introduces an intra-atomic electron-electron interaction as an on-site correction in order to describe systems with localized *d* states, which can produce better band gap relative to GGA method.[43] In previous work, we have calculated U value dependent band gap, and found that the band gap with U=6.6 eV was close to real band gap and also didn't induce unphysical results.[44] Meanwhile, this U value has also been tested by other group.[45] Thus, to account for the strongly correlated interactions of the Ti 3*d* electrons, a moderate on-site Coulomb repulsion U=6.6 eV was applied to the further calculations of electronic structures and optical properties in present work.[46] All parameters, such as k-point and cut off energy are same to the structural optimization.

To calculate the electronic structures and optical properties of pure and C, Ag-codoped anatase TiO_2, the supercell was used, which contained 72 atoms. The substitution method was taken into account in this paper. Our study was based on a supercell with 72 atoms, as a 2×3×1 repetition of the primitive anatase unit cell. For the C, Ag-codoped anatase TiO_2, different numbers O atom were replaced with C atom, and one Ti atom was replaced with Ag atom. Substitution models were formed with configurations of $Ti_{23}O_{47}C_1Ag_1$, $Ti_{23}O_{46}C_2Ag_1$, and $Ti_{23}O_{45}C_3Ag_1$. Substitution models were presented in Fig.1.

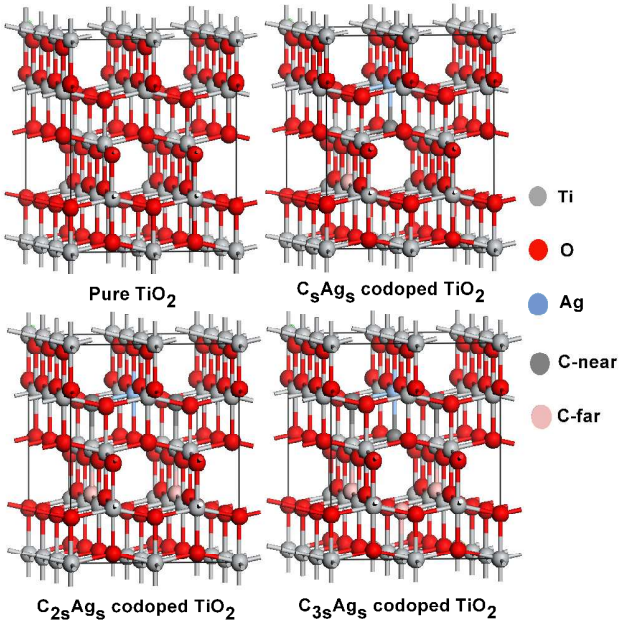

Fig.1 Pure and substitution models of C_sAg_s, $C_{2s}Ag_s$, and $C_{3s}Ag_s$-codoped TiO_2.

Results and Discussions

To evaluate the feasibility of codoped systems, the optimization, lattice distortion, and formation energies have been carried out. We firstly checked the structural properties of C_sAg_s, $C_{2s}Ag_s$, and $C_{3s}Ag_s$-codoped TiO_2. Table 1 gave the lattice parameter *a* and *c* of pure and codoped TiO_2 systems. For pure TiO_2, the lattice constants were 3.776 Å for a and 9.486 Å for *c*, which was very close to the other calculation and experimental data.[47-49] After doping, the *a* and *c* were 3.815 and 9.845 Å for the far C_sAg_s codoped TiO_2, while 3.673 and 10.390 Å were for the near C_sAg_s codoped TiO_2, respectively. Furthermore, the lattice constant *a* increased to 3.941 and 3.959 Å for the far $C_{2s}Ag_s$ and C_3Ag_s codoped TiO_2, while decreased to 3.648 and 3.638 Å for the near $C_{2s}Ag_s$ and C_3Ag_s codoped TiO_2. Generally, it could be seen that the far distance codoping induced less lattice distortion than that of the near distance codoping. Meanwhile, the C_sAg_s codoping suffered less lattice distortion at C low concentration. However, with the increase of C doping concentration, *c* increased sharply. It is indicated that the high concentration may induce large lattice distortion and potential instability.

Table I. Calculated lattice constant of TiO_2,and C_sAg_s, $C_{2s}Ag_s$, and $C_{3s}Ag_s$-codoped TiO_2.

	a (Å)	*c* (Å)
Pure TiO_2	3.776	9.486
C_sAg_s far	3.815	9.845
C_sAg_s near	3.673	10.390
$C_{2s}Ag_s$ far	3.941	10.042
$C_{2s}Ag_s$ near	3.648	10.591
$C_{3s}Ag_s$ far	3.959	10.146
$C_{3s}Ag_s$ near	3.638	10.691

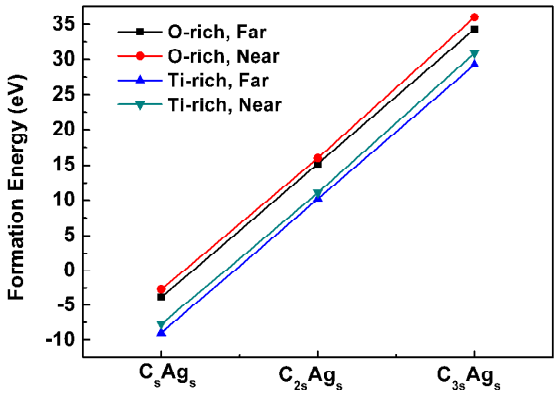

Fig.2 Formation energies of C_sAg_s, $C_{2s}Ag_s$, and $C_{3s}Ag_s$-codoped TiO_2 under Ti-rich and O-rich conditions.

Now, we continue to check the formation energy. For a supercell, the formation energy of doped system is defined as:[41, 50-52]

$$E_f = E_{(\text{codoped})} - E_{(\text{pure})} - n\mu_c - \mu_{Ag} + n\mu_o + \mu_{Ti}$$

where $E_{(\text{codoped})}$ and $E_{(\text{pure})}$ are the total energies of codoped system and pure TiO_2. The *n* is doping atom number. The μ is chemical potential for atom and it was obtained by calculating stable element. We calculated the formation energies of O-rich and Ti-rich conditions. Under Ti-rich condition, it could be seen that formation energies of the far and near C_sAg_s codoped TiO_2 were -8.96 and -7.69 eV, respectively. As a contrast, under O-

rich condition, formation energies were -3.82 and -2.7 eV corresponding to the far and near C_sAg_s codoped TiO_2, respectively. The negative value of formation energy indicated high stability. However, with the increase of C doping concentration, the formation energy sharply increased. The formation energies of the far and near $C_{2s}Ag_s$ codoped TiO_2 were 15.21 and 16.0 eV under O rich condition and 10.22 and 11.09 eV under Ti-rich condition, respectively. Furthermore, the formation energies of the far and near $C_{3s}Ag_s$ codoped TiO_2 increased to above 30 eV under both of O and Ti rich conditions. It was obvious that stability of codoping system got worse under high doping concentration. Thus, combined the lattice distortion and formation energy, it was found that low concentration C_sAg_s was stable, so we performed the further electronic structure calculation using this model.

We then move to the energy band structure calculation. Fig.3 showed the band structures of the near and far C_sAg_s-codoped TiO_2. It was shown that the band gap of the near C_sAg_s-codoped TiO_2 was 2.81 eV, which was lower than 2.89 eV of pure TiO_2. Meanwhile, doped states could be found in the band gap. As a contrast, the band gap of the far C_sAg_s-codoped TiO_2 was decreased to 2.66 eV. Similarly, some discrete energy could also be found in the band gap. These band gap states are close to the previous reported codoping system, such as N-Cr codoped TiO_2.[53] It is necessary to investigate the electronic states in the gap in detail.

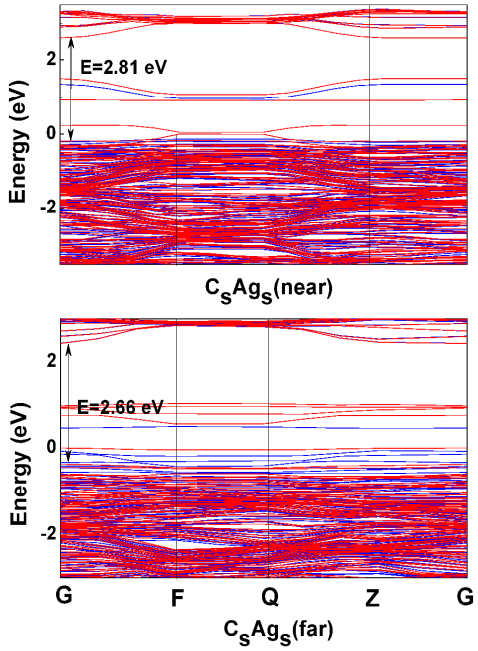

Fig.3 Energy band structure of the near and far C_sAg_s codoped TiO_2. Blue line represents up spin and red line represents down spin.

To explore the electronic states of the pure, near and far distance C_sAg_s codoped TiO_2, we calculated the density of states (DOS), which were presented in Fig.4. Compared with pure TiO_2 (Fig.4a), the C and Ag codoping could induced the mid-gap states in both of the spin-up and the spin-down bands at low C concentration, which mainly composed of the C 2*p* and Ag 4*d* electronic states in the valance band maximum (Fig.4b). Energy level of middle states was deeper for the near distance codoping. Meanwhile, both of the far and near distance codoping induced some C 2*p* states behaving as a part of valance band, which was consistent with previous work. It has been widely reported that C 2*p* states could enhance the electronic states near the valance band.[45] In addition, the spin asymmetry could be observed for the codoped system, but the far codoping was more significant.

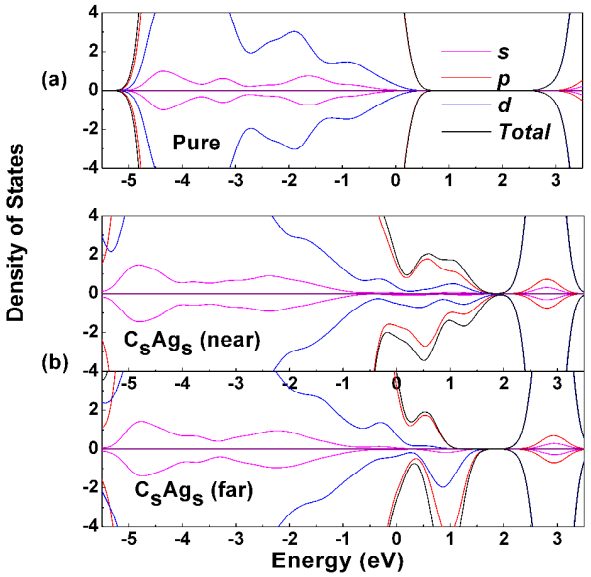

Fig.4 DOS of pure and C_sAg_s-codoped TiO_2.

To investigate the partial density of states (PDOS) of the C_sAg_s codoped system, we further analyzed the Ag 4*d* and C 2*p* states in Fig.5. It was clear that the C 2*p* of the near C_sAg_s codoped TiO_2 showed the very good spin symmetry. As a contrast, the C 2*p* from the far codoped TiO_2 showed the significant spin asymmetry. Meanwhile, Ag 4*d* states from the near codoped TiO_2 also showed better spin symmetry than that of the far codoped TiO_2. It could be concluded that the far distance codoping induced the significant spin asymmetry of C 2*p* and Ag 4*d*.

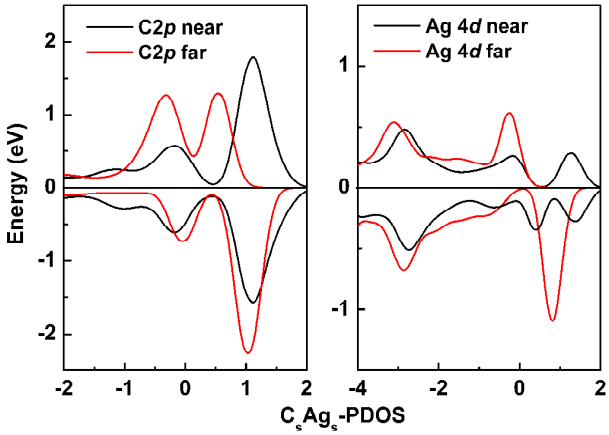

Fig.5 PDOS of the far and near C_sAg_s-codoped TiO_2.

The band gap narrowing was observed for the near and far distance C_sAg_s-codoped systems. The nature of this phenomenon was similar. Combining band structure and DOS, mid-gap states and band gap narrowing were both observed in the two codoped system. However, for the near distance codoping system, middle states were wider and deeper in gap. For the far distance codoping system, as a contrast, middle states were more narrow and induced smaller band gap. Inspired by electronic structure, it is interesting to further investigate the optical properties.

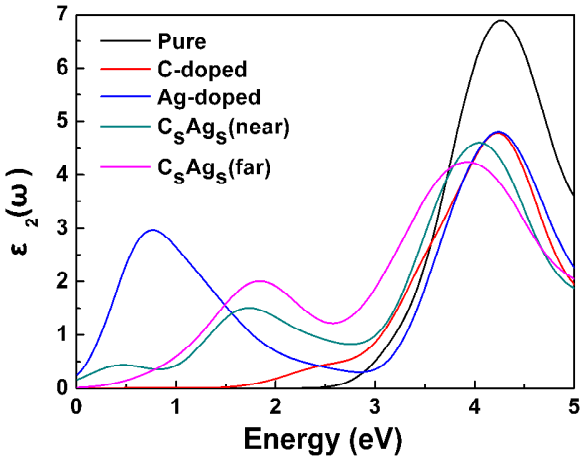

Fig.6 Imaginary parts of dielectric function of pure, single C doped, single Ag doped, and C_sAg_s,-codoped TiO_2.

To investigate the optical transition of C_sAg_s-codoped TiO_2, it is necessary to investigate the imaginary part of the dielectric function (ε_2), because ε_2 is important for describing the optical properties of any materials. Optical transitions between occupied and unoccupied states are caused by the electric field of the photon. The spectra from the excited states can be described as a joint DOS between the valence and conduction bands. Optical transition peaks correspond to optical transition between two states, and the intensity of peaks is proportional to density of states. For the pure TiO_2, 4.29 eV optical transition (Eg) could be only observed (Fig.6). After C and Ag codoping, the optical transition from band gap decreased to 3.92 eV for the far distance C, Ag codoping, and 4.07 eV for the near distance C, Ag codoping. The redshift of the optical transition indicated that the band gaps of C_sAg_s-codoped systems were decreased, which was in good agreement with the result of DOS. Moreover, the optical transition peak around 2 eV could be observed for the C_sAg_s-codoped TiO_2 systems, which indicated that C and Ag codoping could induce visible optical transition. The optical transition peak at 0.4 eV was observed in the near distance C, Ag-codoped TiO_2, but this peak has no contribution to the visible light response. In addition, the optical properties of single C and single Ag doped TiO_2 were also performed. It was found that C and Ag codoping could produce a synergy effect which could further increase the visible absorption compared with the single doping. Especially, the far distance codoping showed the stronger intensity of visible optical transition compared to the near distance codoping, which was interesting. It is necessary to investigate the visible absorptions of the codoped systems.

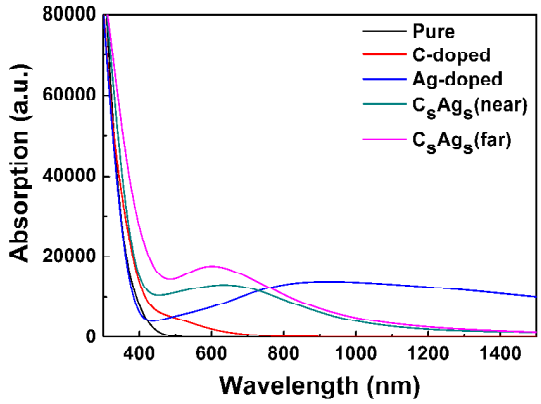

Fig.7 Optical absorption of pure, single C doped, single Ag doped, and C_sAg_s,-codoped TiO_2

Fig.7 presented the optical absorptions of pure, single C doped, single Ag doped, and C_sAg_s,-codoped TiO_2. It was shown that the optical band edges of single C doped and C_sAg_s-codoped TiO_2 shifted to the visible light region compared to the pure TiO_2. It is well known that relation between optical band gap and the absorption coefficient is given by[54-55]

$$\alpha h\nu = c(h\nu - E_g)^{1/2},$$

where h is Planck's constant, c is a constant for a direct transition, ν is frequency of radiation and α is the optical absorption coefficient. The optical band gap E_g can be obtained from the intercept of $(\alpha h\nu)^2$ versus photon energy ($h\nu$). By using the extrapolation, optical band gap of C_sAg_s-codoped system can be obtained. It was found that the calculated optical band gaps decreased from 3.27 eV for pure TiO_2 to 2.68 eV for the far distance C, Ag-codoped TiO_2, and 3.0 eV for the near C, Ag-codoped. The optical band gap of the single C-doped TiO_2 also had a decrease, while the single Ag-doped TiO_2 had not. Meanwhile, the optical absorptions between 450-800 nm were enhanced for both of the near and far codoped systems compared with the pure and single doped TiO_2. Especially, the absorption intensity of the far distance codoped TiO_2 was obviously higher than that of the near distance codoped TiO_2. We calculated the optical properties of N, B-codoped TiO_2 by using GGA+U method, and found visible absorption was in the range of 400-700 nm. It was also found that the C-doped TiO_2 could form the localized states and thus induced the significant visible optical absorption.[28] Besides, the recent investigation also showed the B, Ag-codoped TiO_2 could present the stronger visible light absorption in the range of 400-800 nm than that of B or Ag single doped TiO_2.[56] Our work used GGA+U method to correct the band gap and clearly showed that the visible optical absorption of C, Ag-codoped TiO_2 should be reliable. Importantly, C and Ag codoping induced the synergy effect both for the far distance codoping and near distance codoping.

Conclusion

In summary, the electronic structures and optical properties of the single C doped, single Ag doped , and C, Ag-codoped TiO_2

were calculated based on the GGA+U method. It was found that the far and near distance codoping both induced the band gap narrowing and visible optical absorption, and C and Ag codoping could produce obvious synergy effect compared with the single C and single Ag doping. After codoping, the visible absorption in the 450-800 nm was sharply increased, moreover, the far distance codoping induced more significant band gap narrowing and visible optical absorption. Therefore, it is conceived that the C, Ag-codoped TiO_2 should be helpful for visible photoactivity.

Acknowledgments

Author would like to thank Prof. Yanni Li, School of Chemical Engineering and Technology at Tianjin University, for providing us with the computational plat. This work is supported by the National Natural Science Foundation of China (Grant No. 11304220)

Notes

[a] *Department of Physics, School of Science, Tianjin Chengjian University, Tianjin, 300384, China*

References:

1 A. L. Linsebigler, G. Lu, J. T. Yates Jr, *Chem.Rev.*, **1995,** *95*, 735-758.
2 S. U. Khan, M. Al-Shahry, W. B. Ingler, *Science*, **2002,** *297*, 2243-2245.
3 S. Song, B. Y. Xia, J. Chen, J. Yang, X. Shen, S. Fan, M. Guo, Y. Sun, X. Zhang, *RSC Adv.*, **2014**,4, 42598–42603.
4 T. Umebayashi, T. Yamaki, H. Itoh, K. Asai, *Appl. Phys. Lett.*, **2002,** *81*, 454-456.
5 R. Asahi, T. Morikawa, T. Ohwaki, K. Aoki, Y. Taga, *Science*, **2001,** *293*, 269-271.
6 J. Yu, Q. Xiang, M. Zhou, *Appl.Catal.B:Environ.,* **2009,** *90*, 595-602.
7 M. Guo, X. Zhang, C. Liang, *Physica B*, **2011,** *406*, 3354-3358.
8 M. L. Guo, X. D. Zhang, C. T. Liang, G. Z. Jia, *Chin Phys Lett*, **2010,** *27*, 057103.
9 K. Yang, Y. Dai, B. Huang, *J. Phys. Chem. C*, **2007,** *111*, 12086-12090.
10 S. Hoang, S. P. Berglund, N. T. Hahn, A. J. Bard, C. B. Mullins, *J. Am. Chem. Soc.*, **2012,** *134*, 3659-3662.
11 F. Spadavecchia, G. Cappelletti, S. Ardizzone, M. Ceotto, L. Falciola, *J. Phys. Chem. C*, **2011,** *115*, 6381-6391.
12 R. Long, N. J. English, *Appl. Phys. Lett.*, **2009,** *94,* 132102.
13 M. Harb, P. Sautet, P. Raybaud, *J. Phys. Chem. C*, **2011,** *115*, 19394-19404.
14 Z. Lin, A. Orlov, R. M. Lambert, M. C. Payne, *J. Phys. Chem. B*, **2005,** *109*, 20948-20952.
15 J. Tao, L. Guan, J. Pan, C. Huan, L. Wang, J. Kuo, Z. Zhang, J. Chai, S. Wang, *Appl. Phys. Lett.,* **2009,** *95*, 06250.
16 J. Yu, P. Zhou, Q. Li, *Phys. Chem. Chem. Phys.*, **2013,** *15*, 12040-12047.
17 F. Dong, S. Guo, H. Wang, X. Li, Z. Wu, *J. Phys. Chem. C*, **2011,** *115*, 13285-13292.
18 X. Chen, C. Burda, *J. Am. Chem. Soc.*, **2008,** *130*, 5018-5019.
19 W. Choi, A. Termin, M. R. Hoffmann, *J. Phys. Chem.*, **1994,** *98*, 13669-13679.
20 X. Zhang, M. Guo, C. Liu, W. Li, X. Hong, *Appl. Phys. Lett.*, **2008,** *93*, 012103.
21 M. Guo, J. Du, *Physica B*, **2012,** *407*, 1003-1007.
22 B. Liu, H. M. Chen, C. Liu, S. C. Andrews, C. Hahn, P. Yang, *J. Am. Chem. Soc.*, **2013,** *135*, 9995-9998.
23 Y. Ni, Y. Zhu, X. Ma, *Dalton Trans.*, **2011,** *40*, 3689-3694.
24 S. In, A. Orlov, R. Berg, F. García, S. Pedrosa-Jimenez, M. S. Tikhov, D. S. Wright, R. M. Lambert, *J. Am. Chem. Soc.*, **2007,** *129*, 13790-13791.
25 J. Zhang, Y. Wu, M. Xing, S. A. K. Leghari, S. Sajjad, *Energy Environ. Sci.*, **2010,** *3*, 715-726.
26 Y.-F. Li, D. Xu, J. I. Oh, W. Shen, X. Li, Y. Yu, *ACS Catal.*, **2012,** *2*, 391-398.
27 H. Kato, A. Kudo, *J. Phys. Chem. B*, **2002,** *106*, 5029-5034.
28 Y. Gai, J. Li, S.-S. Li, J.-B. Xia, S.-H. Wei, *Phys.Rev.Lett.*, **2009,** *102*, 036402.
29 L. Mi, P. Xu, H. Shen, P.-N. Wang, W. Shen, *Appl. Phys. Lett.,* **2007,** *90*, 171909.
30 J. Zhang, C. Pan, P. Fang, J. Wei, R. Xiong, *ACS Appl. Mater. Interfaces*, **2010,** *2*, 1173-1176.
31 W. Zhu, X. Qiu, V. Iancu, X.-Q. Chen, H. Pan, W. Wang, N. M. Dimitrijevic, T. Rajh, H. M. Meyer, M. P. Paranthaman, G. M. Stocks, H. H. Weitering, B. Gu, G. Eres, Z. Zhang, *Phys.Rev.Lett.*, **2009,** *103*, 226401.
32 M. E. Kurtoglu, T. Longenbach, K. Sohlberg, Y. Gogotsi, *J. Phys. Chem. C*, **2011,** *115*, 17392-17399.
33 L. Huang, A. Rosa, R. Ahuja, *Phys. Rev. B*, **2006,** *74*, 075206.
34 W.-J. Yin, S.-H. Wei, M. M. Al-Jassim, Y. Yan, *Phys.Rev.Lett.*, **2011,** *106*, 066801.
35 M. Guo, X.-D. Zhang, J. Du, *Phys. Status Solidi RRL,* **2012,** *6*, 172-174.
36 N. Feng, A. Zheng, Q. Wang, P. Ren, X. Gao, S.-B. Liu, Z. Shen, T. Chen, F. Deng, *J. Phys. Chem. C*, **2011,** *115*, 2709-2719.
37 D. Carroll, P. Redlich, X. Blase, J.-C. Charlier, S. Curran, P. Ajayan, S. Roth, M. Rühle, *Phys Rev Lett*, **1998,** *81*, 2332.
38 J. P. Perdew, K. Burke, M. Ernzerhof, *Phys.Rev.Lett.*, **1996,** *77*, 3865.
39 M. C. Payne, M. P. Teter, D. C. Allan, T. Arias, J. Joannopoulos, *Rev.Mod. Phys.*, **1992,** *64*, 1045-1097.
40 H. J. Monkhorst, J. D. Pack, *Phys. Rev. B*, **1976,** *13*, 5188-5192.
41 R. Long, N. J. English, *Chem. Phys. Lett.*, **2009,** *478*, 175-179.
42 L. Li, W. Wang, H. Liu, X. Liu, Q. Song, S. Ren, *J. Phys. Chem. C*, **2009,** *113*, 8460-8464.
43 V. I. Anisimov, F. Aryasetiawan, A. Lichtenstein, *J.Phys.: Condens. Matter*, **1997,** *9*, 767-808.
44 M. Guo, J. Du, *Int. J. Mod. Phys. B*, **2013,** *27*, 1350123.
45 K. Yang, Y. Dai, B. Huang, M.-H. Whangbo, *J. Phys. Chem. C*, **2009,** *113*, 2624-2629.
46 H. J. Kulik, M. Cococcioni, D. A. Scherlis, N. Marzari, *Phys.Rev.Lett.*, **2006,** *97*, 103001.
47 S. Na-Phattalung, M. F. Smith, K. Kim, M.-H. Du, S.-H. Wei, S. Zhang, S. Limpijumnong, *Phys.Rev.B*, **2006,** *73*, 125205.
48 A. Janotti, J. Varley, P. Rinke, N. Umezawa, G. Kresse, C. Van de Walle, *Phys.Rev.B*, **2010,** *81*, 085212.
49 Y. Wang, H. Liu, Z. Li, X. Zhang, R. Zheng, S. Ringer, *Appl. Phys. Lett.,* **2006,** *89*, 042511.
50 F. Oba, A. Togo, I. Tanaka, J. Paier, G. Kresse, *Phys. Rev. B*, **2008,** *77*, 245202.
51 J. Li, S.-H. Wei, S.-S. Li, J.-B. Xia, *Phys. Rev. B*, **2006,** *74*, 081201.
52 X. Cui, J. Medvedeva, B. Delley, A. Freeman, N. Newman, C. Stampfl, *Phys.Rev.Lett.*, **2005,** *95*, 256404.
53 M. Chiodi, C. P. Cheney, P. Vilmercati, E. Cavaliere, N. Mannella, H. H. Weitering, L. Gavioli, *J. Phys. Chem. C*, **2011,** *116*, 311-318.
54 X. Zhang, M. Guo, W. Li, C. Liu, *J. Appl.Phys.*, **2008,** *103*, 063721.
55 V. Srikant, D. R. Clarke, *J. Appl.Phys.*, **1998,** *83*, 5447.
56 N. Feng, Q. Wang, A. Zheng, Z. Zhang, J. Fan, S.-B. Liu, J.-P. Amoureux, F. Deng, *J. Am. Chem. Soc.*, **2013,** *135*, 1607-1616.